Desalination and Water Treatment
www.deswater.com

doi: 10.1080/19443994.2014.1003102

57 (2016) 5200–5211
March

Taylor & Francis
Taylor & Francis Group

Removal of a common textile dye, navy blue (NB), from aqueous solutions by combined process of coagulation–flocculation followed by adsorption

H. Nourmoradi[a], S. Zabihollahi[b], H.R. Pourzamani[c,*]

[a]*Department of Environmental Health Engineering, School of Health, Ilam University of Medical Sciences, Pajouhesh Ave, Banganjab, Ilam, Iran, Tel. +988412235733; email: Ilam_nourmoradi@yahoo.com*
[b]*Department of Environmental Health Engineering, Environment Research Center, Student Research Center, School of Health, Isfahan University of Medical Sciences, Hezar Jerib Ave, Isfahan, Iran, Tel. +983137922668; email: S.zabihollahi@yahoo.com*
[c]*Department of Environmental Health Engineering, Environment Research Center, School of Health, Isfahan University of Medical Sciences, Hezar Jerib Ave, Isfahan, Iran, Tel./Fax: +983136682509; email: Pourzamani@hlth.mui.ac.ir*

Received 11 June 2014; Accepted 21 December 2014

ABSTRACT

The decolorization and removal of chemical oxygen demand (COD) of a textile dye, Navy blue CE-RN (NB), were investigated from aqueous solutions by combined process of coagulation–flocculation(C–F) and adsorption. Common coagulants (alum, lime, poly aluminum chloride (PACl), and ferric chloride) and clay [montmorillonite (Mt) and nano-montmorillonite (NMt)] were used in C–F and adsorption steps, respectively. The maximum COD and dye removal was observed by coagulant of PACl in the C–F process. The optimum conditions for dye removal by PACl were occurred by coagulant dose of 0.1 g/L at pH 6. In the adsorption process, the optimum contact times of 120 and 20 min were obtained for Mt and NMt, respectively. The findings indicated that the optimum conditions for the dye sorption were observed at pH 2 and the adsorbent dose 1.8 g/L. The sorption data also showed that the adsorption of NB onto the sorbents was better followed the pseudo-second order kinetic models. The dye and COD concentrations during the combined treatment process were decreased from 300 to 2–4.5 mg/L and from 732 to 2–35 mg/L, respectively. This indicates that the combined process of C–F followed by adsorption can be used as a proper alternative for the treatment of NB dye-containing wastewaters.

Keywords: Aqueous solution; Dye; Coagulation; Flocculation; Adsorption

1. Introduction

In recent decades, industries have been considered as one of the main factors of environmental pollution, especially in developing countries [1]. Many industries such as textile, carpet, cosmetic, pulp, and paper discharge huge amounts of pollutants including dye materials into the aquatic environment [2–5]. About 30% of dyes consumed in the abovementioned industries are unstable during the dying process and are discharged directly into the wastewater [6]. Therefore, the colored wastewaters that produced from these industries are remarkable [7]. Dyes have diverse structures such as disperse, acidic, basic, anthraquinone, azo, diazo based and metal complex dyes [8]. Disperse

*Corresponding author.

dyes are one of the most common types of textile dyes that contain high organic matter as chemical oxygen demand (COD) [9,10]. Disperse dyes-containing wastewaters have extensive harmful effects on the human health as well as aquatic organisms. Many of these dye compounds have toxic, mutagenic, carcinogenic, and teratogenic effects, and they can cause allergy, dermatitis, and skin irritation in human [3,5,11,12]. Due to these harmful effects, the colored wastewaters must be appropriately treated before discharging into the water resources and ecosystem. Several processes including coagulation–flocculation, electro-coagulation, adsorption, advanced oxidation processes (O_3/H_2O_2, H_2O_2/UV and photo-catalysis), flotation, membrane techniques (ultra-filtration, nanofiltration, and reverse osmosis), and biological degradation have been successfully applied for dyes removal from wastewaters [5,6,10,11,13–15]. Despite a series of advantages, there are some disadvantages and limitations such as low removal efficiency, great electrical energy requirement, and high-cost operation for the various dye treatment methods [4,16]. The C–F technique is a principal process to treat the colored wastewaters from textile industries [12,17]. Generally, the C–F process is a suitable technology with low installation cost and significant efficiency [18]. Many studies, Table 1, have been carried out by C–F process on the COD and color removal from textile wastewaters [10,13,19]. As seen, C–F process has low removal efficiency for some dyes [12]. So, this process can be combined with the other treatment processes to enhance dye removal from wastewater. Among the various methods, adsorption process, because of high removal efficiency, simplicity and extensive utilization, is an appropriate technique to remove dye pollutants from aqueous media [14,20–23]. In recent years, many studies have been conducted on the dye adsorption by different absorbents such as fly ash, peat, wood powder, coir pith, lignin, clay, bottom ash, zeolite, calcine alunite, peanut hull, rice husk, brown seaweed, cellulose, silica gel, bagasse pith, maize cob, orange peel, and waste red mud [2,11,16,20,21,24,25]. Because of high abundance, availability, non-toxicity, low cost and large specific surface area, clay mineral is an attractive adsorbent to remove various dyes from wastewaters [2,5,16,26,27]. The combination of C–F technique with adsorption process cause high efficiency of dye removal, less produced sludge, coagulant savings, and economic feasibility [28,29]. The aim of this work was to investigate the color and COD removal from a disperse dye (NB)-containing solution through combined process of C–F followed by adsorption with clay and nanoclay. To the best of our knowledge, some studies about these combined treatment method have been carried out to remove other types of dyes including reactive dyes from aqueous solutions [28–31]. This study determines the best coagulant type and optimum pH for the removal of dye and COD in C–F step and specifies the optimum adsorption conditions (pH, contact time, adsorbent dose) in the adsorption step. Various dye desorption procedures have been also carried out on the spent (dye-saturated) adsorbent to find out the best method for the regeneration of sorbent.

2. Materials and methods

2.1. Materials

The clay minerals including montmorillonite (Mt) and nanomontmorillonite (NMt) were purchased from Laviosa Co (Italy) and Southern clay product Co (USA), respectively. The commercial textile dye, Navy blue CE-RN (NB), was obtained from Setapers Co (Turkey) and was used without additional purification. The commercial grade of lime ($Ca(OH)_2$), alum (Al_2 $(SO_4)_3.18$ H_2O), and PACl was supplied from Behinab Co (Iran). Other analytical grade chemicals, NaOH (98%), H_2SO_4 (95–97%), $FeCl_3{\cdot}6H_2O$ (99%), CaCl2, ethanol (95–96%) were provided from Merck Co (Germany).

2.2. Characterization and analysis

Table 2 shows the physiochemical properties of the adsorbents [1]. The spectra and compositions of the adsorbents were specified by Fourier transform infrared spectrophotometer (FTIR, JASCO, FT/IR-6300, Japan) and X-ray diffractometer (XRD) (Bruker, D8 ADVANCE, Germany, using Ni filtered Cu Kα

Table 1
COD and dye removal from textile wastewaters by C–F process

Type of coagulant	Type of dye	Color removal (%)	COD removal (%)	References
Ferric chloride	Reactive	12.0	66.0	[19]
Aluminum sulfate	Direct	50.0	50.0	[19]
Ferric chloride	Reactive	60.9	26.5	[13]
Ferric chloride	Reactive	60.9	25.0	[10]

Table 2
The compositions of Mt and NMt in this study

Chemical compounds	Compounds percent in adsorbents (%)	
	Clay (Mt)	Nanoclay (NMt)
SiO_2	60.00	61.90
Al_2O_3	20.03	21.06
Fe_2O_3	2.31	4.83
Na_2O	3.02	4.15
P_2O_5	0.05	0.00
MgO	4.02	2.22
K_2O	0.13	0.06
CaO	1.46	0.16
TiO_2	0.24	0.13
MnO	0.03	0.00
H_2O	8.71	5.49
Other		
CEC (meq/100 g)	108	80
Limit of ignition (%)	7.03	6.80

radiation 1.5406 Å), respectively. Also, COD content of the dye solutions was measured using closed reflux, titrimetric method [32], and the concentration of NB dye in the solutions was determined by spectrophotometric method (UV/Vis, LANGE, Hatch Co.,) at the maximum absorbance wavelength (473 nm). The dye and COD removal efficiency and the adsorption capacity (q_e) were calculated by the following equations:

$$\text{Dye or COD removal } (\%) = \frac{C_i - C_s}{C_i} \times 100 \quad (1)$$

$$q_e = \frac{(C_i - C_s)V}{m} \quad (2)$$

where C_i (mg/L) is the initial dye or COD quantity, C_s (mg/L) is the dye or COD quantity after treatment process. V (L) and m (g) are the solution volume and adsorbent mass, respectively.

2.3. Experiments

All the experiments were conducted at room temperature (25˚C). The experiments were performed in duplicates and the average values were considered.

2.3.1. Coagulation–flocculation tests

A six beaker jar-test apparatus (Philips & Bird Stirrer Model 7790-402) was used for C–F experiments. The effect of various coagulants doses (0–1 g/L of alum, ferric chloride and PACl and 0–7.5 g/L of lime) and solution pH was determined on the C–F process via measuring COD and dye content of the samples. The coagulation and flocculation were conducted at mixing speed of 180 rpm for 2 min and at 40 rpm for 15 min, respectively. A settling time of 30 min was also used after C–F process to remove sludge from the solution. A stock solution (300 mg/L) of dye was synthetically prepared with distilled water, and one liter of the solution was transferred into each Plexiglas beaker. The stock solution contained 732 mg/L COD resulting from dye. After conducting the treatment process, the sample was taken at 3 cm below the effluent surface to determine the dye and COD removal efficiency. In order to evaluate the removal efficiency of dye and COD through the combined treatment process (C–F followed by adsorption), the supernatant obtained from C–F process was used for the adsorption experiments.

2.3.2. Adsorption experiments

All the adsorption experiments were carried out in batch system with 0.1 g adsorbent into 100 mL dye effluent in 250 mL Erlenmeyer flasks sealed with cape. The suspensions were mixed by an orbital shaker (250 rpm). The effect of various parameters such as contact time (0–4 h), pH (2–10), adsorbent dose (0.02–0.2 g/L), and solution ion strength (20–100 mg/L Ca^{+2}) was determined on the adsorption. After sorption process, the suspensions were centrifuged (6,000 rpm for 10 min) and the clear supernatants were analyzed to determine COD and color content.

2.3.3. Regeneration of dye-saturated adsorbent

After adsorption experiments, the dye-saturated adsorbents were collected by centrifugation (6,000 rpm at 15 min) and dried in an oven at 40˚C for 24 h. The saturated sorbents were then ground and sieved through a 125-μm sieve. Three regeneration techniques including chemical, ultrasonic, and thermal were conducted for desorption of dye-saturated sorbents. Subsequently, the adsorption was conducted by the regenerated sorbents similar to the original adsorbents to determine the regeneration efficiency.

2.3.3.1. Chemical regeneration. Chemical regeneration was performed by NaOH, KOH, H_2SO_4, and acetic acid solutions (1 N). Initially, 1 g of dye-saturated adsorbent was separately placed into 50 mL of each desorption solution in 100 mL Erlenmeyer flasks. The flasks were

then mixed by a rotary shaker (at 250 rpm and contact times of 120 min and 20 min for Mt and NMt, respectively). The sorbent was finally rinsed with distilled water to constant pH and was dried at 40˚C.

2.3.3.2. Ultrasonic regeneration. First, 1 g of colored adsorbent was introduced into 50 mL of ethanol (95–96%) in 100 mL Erlenmeyer flask, and the sample was then located in an ultrasonic bath (BANDELIN electronic, DT156, Power:160–640 W, frequency: 35 KHz) for 15 min. The sorbent was then washed with distilled water and was dried at 40˚C.

2.3.3.3. Thermal regeneration. Thermal regeneration was carried out by placing 1 g dye-saturated adsorbent into 50 mL hot water (95 ± 0.5˚C) in a 100 mL beaker for 15 min. Another thermal regeneration method was conducted by dry heating through an experimental oven at 300˚C for 15 min.

3. Results and discussion

3.1. Coagulation–flocculation experiments

3.1.1. Effect of coagulant dose

The influence of various doses of coagulants (alum, lime, ferric chloride, and PACl) was investigated to remove dye and COD of the dye-containing solutions with fixed NB concentration (300 mg/L) at natural pH of dye (pH 6). The removal efficiency of different coagulants was presented in Fig. 1. As seen, PACl with the coagulant dose of 0.1 g/L had the highest

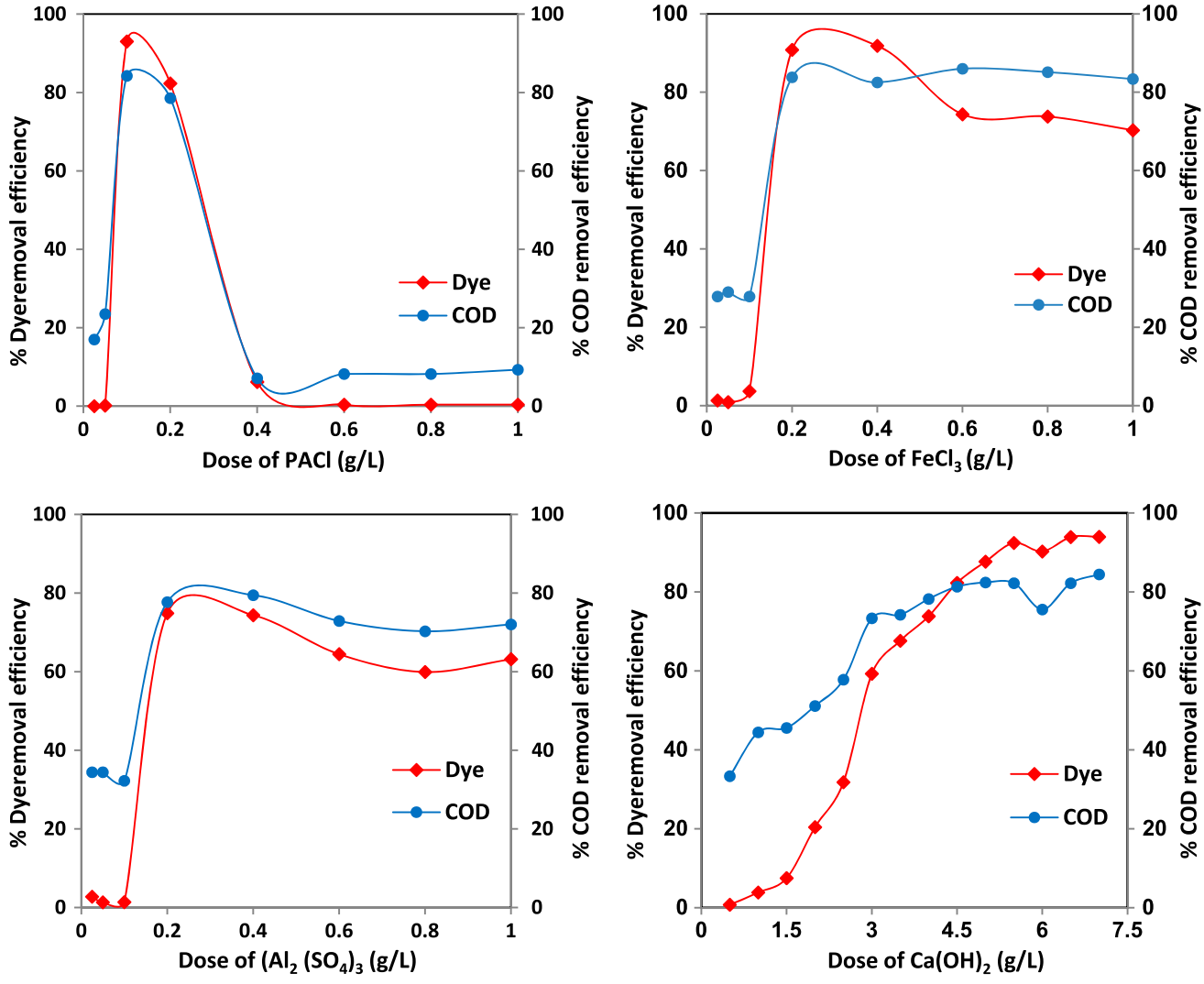

Fig. 1. Influence of different doses of coagulants on the removal of dye and COD (dye concentration = 300 mg/L and pH 6).

removal efficiency (84.26% COD removal and 93.03% dye removal) in comparison with other used coagulants. Alum with dose of 0.2 g/L removed 77.70% COD and 74.88% dye. Lime (4.5 g/L) and ferric chloride (0.4 g/L) also had COD removal efficiency of 81.33 and 82.51%, and color removal of 82.28 and 91.85%, respectively.

3.1.2. Determination of optimum pH for coagulation

The solution pH plays an important role in coagulation process. Therefore, the effect of solution pH (2–10) on the dye and COD removal was measured at the optimum coagulants dose (Fig. 2). As shown, the best solution pH for the maximum removal of dye and COD using PACl was occurred at pH 6. But, the maximum dye and COD removal was found to be at pH 10 for other coagulants. The dye and COD removal efficiency by PACl at the optimum coagulant dose (0.1 g/L) and pH (pH 6) was 93.03 and 84.26%, respectively. Kumar et al. (2008) reported that the optimum solution pH for dye removal by PACl was occurred at pH 4 [17]. Wen et al. (2003) also showed that the maximum dye removal (a disperse dye, Terasil Blue BGE-01) with PACl coagulant was happened at solution pH 4–5 and coagulant dose of 0.2 g/L [33]. The maximum dye and COD removal by alum and ferric chloride was taken place at pH 10. This phenomenon is probably due to the formation of metallic hydroxide precipitates that they provide adsorptive coagulating mechanisms to entrap the impurities [34–36]. Disperse dye has low solubility in water [10]. Therefore, the dye can be adsorbed and flocculated by the formed precipitates and then it helps to form flocs [10,13,36]. The removal efficiency of dye and COD at the optimum coagulant dose and pH was as follows: alum = 74.88%, 77.7%, ferric chloride = 91.85%, 82.51% and lime = 82.28%, 81.33%, respectively. The colored supernatant of PACl (more efficient coagulant) was applied for the sorption studies in the subsequent experiments.

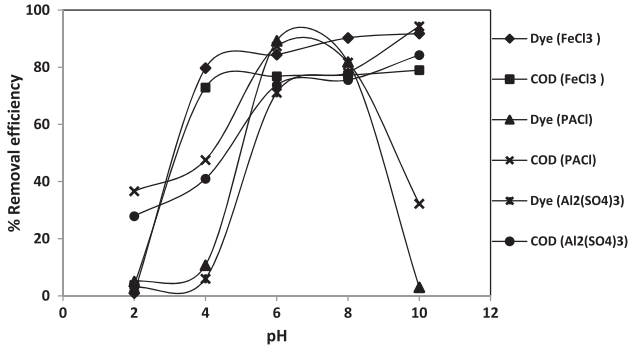

Fig. 2. Determination of the optimum pH value for the removal of dye and COD by coagulants (dye concentration = 300 mg/L, coagulant concentrations; alum = 0.2 g/L, ferric chloride = 0.4 g/L, and PACl = 0.1 g/L).

3.2. Characterization of adsorbents

The X-ray diffraction (XRD) patterns of raw and colored adsorbents are presented in Fig. 3. As seen, the peaks intensity of the dye-contained Mt and NMt was increased. The XRD patterns list showed that copper and sulfur compounds were found as the components of the colored adsorbents. But, these compounds were not found in the chemical composition

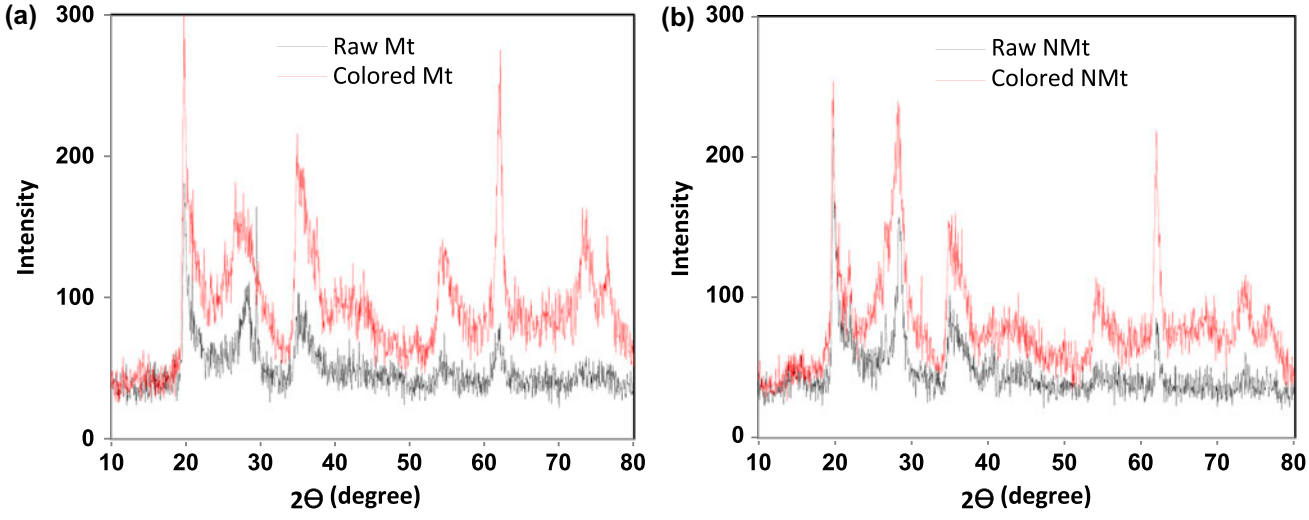

Fig. 3. The XRD patterns of (a) Mt and (b) NMt.

list of the raw adsorbents (Table 2). Based on these observations, it can be concluded that the presence of copper and sulfur compounds in the XRD patterns of colored adsorbents may be due to the sorption of NB by the sorbents.

The FTIR technique was also used to recognize the interaction between adsorbate and the functional groups of the adsorbents [37]. Fig. 4 shows the FTIR spectrum of the raw and colored adsorbents. The absorption peak around 3,436 cm^{-1} may be due to the vibrations of N–H groups [38]. The peak at 3,400 $cm^{-1}$is usually due to stretching vibration of hydroxyl (OH) functional groups [39,40].The new band at 1,692 cm^{-1} in the colored adsorbents can be assigned to C=O groups as a result of NB adsorption [40,41]. The stretching regions of 2,925 cm^{-1} (asymmetric) and 2,850 cm^{-1} (symmetric) are also attributed to C–H stretch [39,40]. The bands in the 1,550–1,350 cm^{-1} region are allocated to vibrations of $CaCO_3$ compound [40]. The broad band in the range of 1,000–1,300 cm^{-1} in the colored adsorbents (especially in NMt) can be also ascribed to S=O band [39]. It can be concluded from the change in the peaks intensity and also the presence of S=O, C–H, and N–H bonds in the colored adsorbents that NB dye in the solution has been removed by Mt and NMt.

3.3. Adsorption experiments

3.3.1. Effect of contact time

The effect of contact time on the dye and COD removal is shown in Fig. 5. As seen, the sorption capacity was increased by increasing the time up to 120 min and up to 20 min for Mt and NMt, respectively. The uptake capacity by the sorbents was then slightly decreased as time went forward (after peak point). This may be due to the adsorption sites that were abundantly available at the beginning the contact time. But they reduce and saturate over time. The sorption capacity (q_e) and COD removal efficiency for Mt and NMt at the equilibrium times were 8.93 mg/g, 41.51% and 8.87 mg/g, 19.14%, respectively. As can be seen, there was a great time variation between the adsorbents to achieve the equilibrium time, while the sorption capacity of the adsorbents had not significantly difference. This may be due to the nanoscale spacing of NMt inter layers [42]. The optimum contact times of 120 min for Mt and 20 min for NMt were applied for the next sorption experiments in this study.

3.3.1.1. Adsorption Kinetics. The sorption kinetic models are one of the useful parameters to determine the characteristics of adsorption process. Three common kinetic models, pseudo-first order (Eq. (3)), pseudo-second order (Eq. (4)), and intraparticle diffusion (Eq. (5)), were investigated in this study.

$$\ln\,(q_e - q_t) = \ln\,q_e - K_1 t \tag{3}$$

$$\frac{t}{q_t} = \frac{1}{k_2 q_e^2} + \frac{t}{q_e} \tag{4}$$

$$q_t = k_{id} t^{0.5} + C \tag{5}$$

where q_e (mg/g) and q_t (mg/g) are the adsorption capacities of dye at equilibrium and at time (t), respectively. K_1 (1/h), K_2 (g/mg h), and K_{id} (g/mg h)

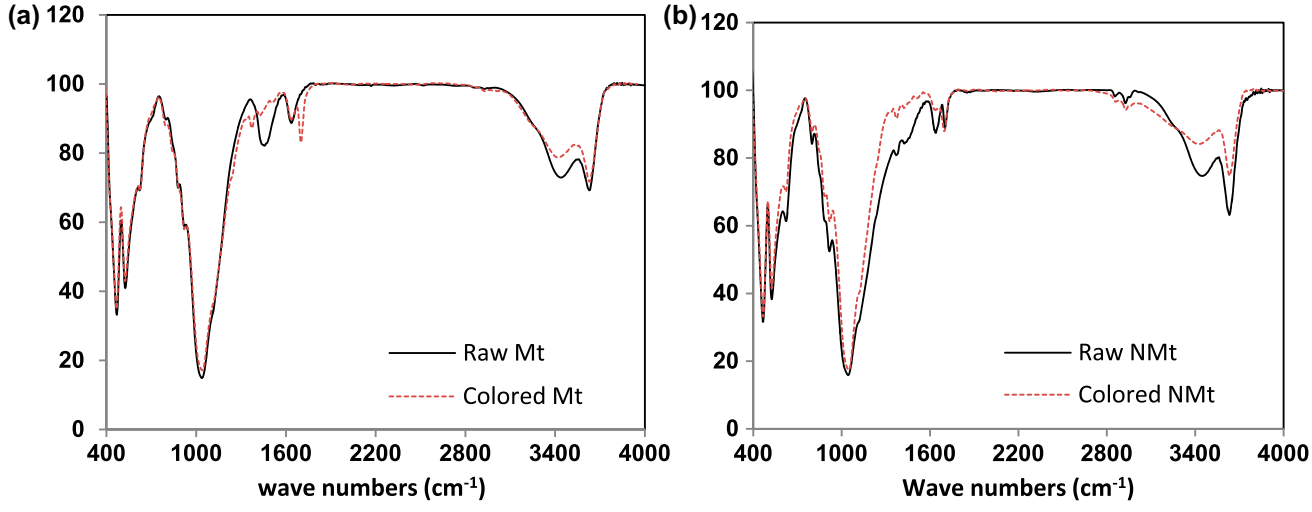

Fig. 4. FTIR spectra of the raw and colored of (a) Mt and (b) NMt.

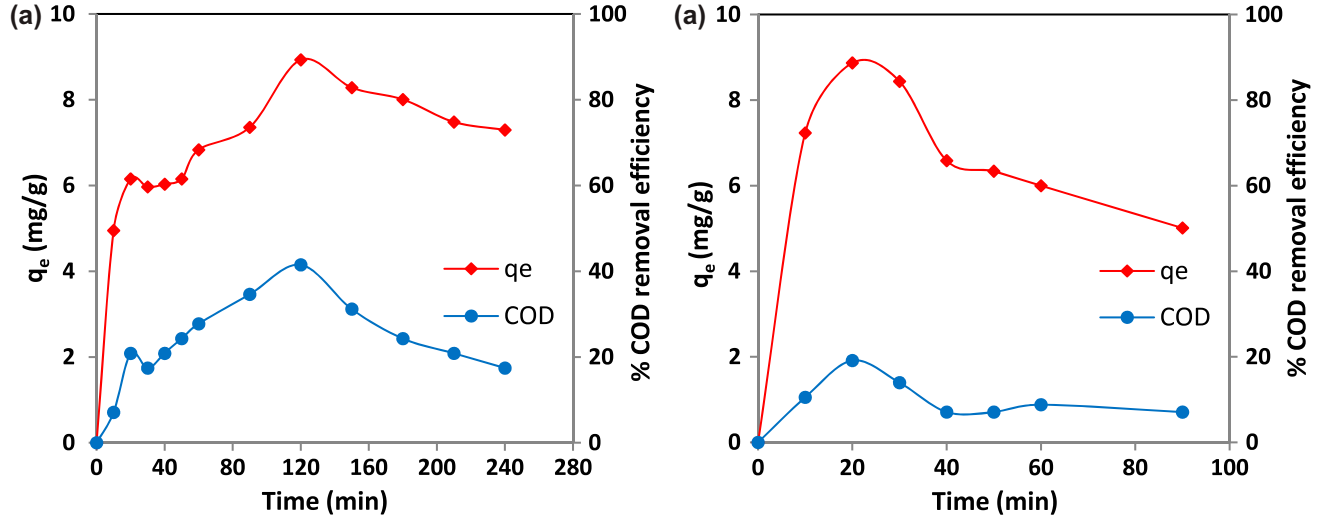

Fig. 5. The effect of contact time on the dye and COD removal by (a) Mt and (b) NMt (at natural pH of samples and 0.1 g adsorbent).

are also the rate constants of the pseudo-first order, pseudo-second order, and intraparticle diffusion models, respectively [1]. The adsorption kinetic models parameters are presented in Table 3. As can be seen, the correlation coefficient (R^2) of the pseudo-second order kinetic model was higher than of other kinetic models. Therefore, the pseudo-second order kinetic model was more appropriate to describe the adsorption of dye onto Mt and NMt. Ho and Chiang (2001) reported similar results for the adsorption of Acid Blue 9 by mixture of activated carbon and activated clay [43]. The pseudo-second order kinetic model for the adsorption of NB by Mt and NMt is presented in Fig. 6. Intraparticle diffusion model was also used to identify the diffusion mechanism of NB onto the sorbents. According to Table 3, the values of the intercept obtained by this kinetic model did not pass via the origin, ($C \neq 0$). Therefore, the intraparticle diffusion was not only kinetic limiting factor in this adsorption process [21].

3.3.2. Effect of pH

The effect of solution pH (2–10) on the dye and COD removal by the adsorbents is shown in Fig. 7. As seen, the dye and COD removal efficiencies were decreased with increasing pH values from 2 to 10. The adsorbents reached the maximum removal efficiency in the acidic conditions (pH 2). This may be due to the electrostatic interaction between adsorbents and dye. At pH 2, high concentration of hydrogen ions can protonate the negative surface of the adsorbents and consequently, the adsorbents surface become more positively charged [44]. This phenomenon can produce the attractive force between NB molecules and positively charged surface of Mt and NMt. Therefore, the dye sorption was lastly increased at pH 2. Otherwise, with increasing solution pH, because of the presence of hydroxyl ions into the solution and repulsive force between OH^- ions and the negative surface of the adsorbents, the sorption capacity was decreased [44]. Hemsas et al. reported that maximum sorption capacity of two disperse dyes (blue palanil and yellow

Table 3
Adsorption kinetic models parameters of obtained from this study

		Pseudo-first-order			Pseudo-second-order				Intraparticle diffusion		
Adsorbent	$q_{e,\ experimental}$	K_1 (1/h)	$q_{e,calculated}$ (mg/g)	R^2	K_2 (g/mg h)	h (g/mg h)	$q_{e,\ calculated}$ (mg/g)	R^2	K_{id} (1/h)	C	R^2
Mt	8.93	0.01	4.22	0.94	0.02	1.81	9.33	0.96	0.43	3.58	0.88
NMt	8.87	0.02	1.28	0.45	0.09	2.02	4.74	0.98	0.51	10.13	0.63

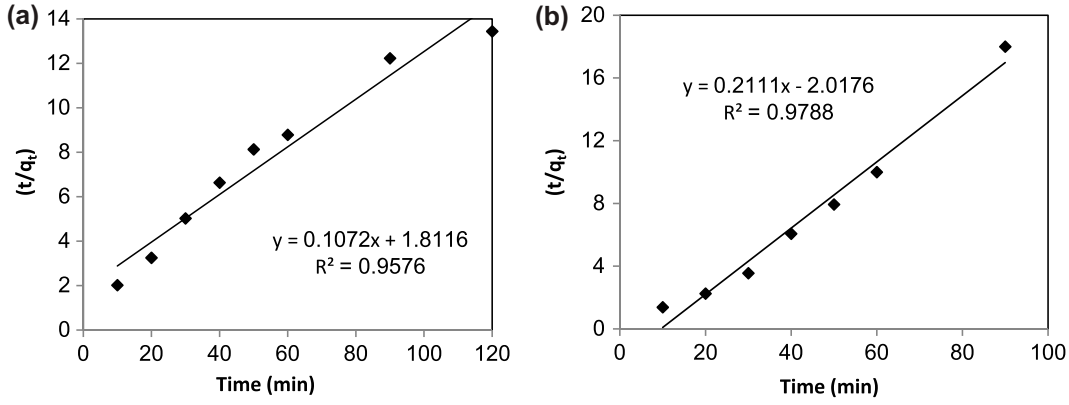

Fig. 6. Plot of pseudo-second order kinetic model for (a) Mt and (b) NMt.

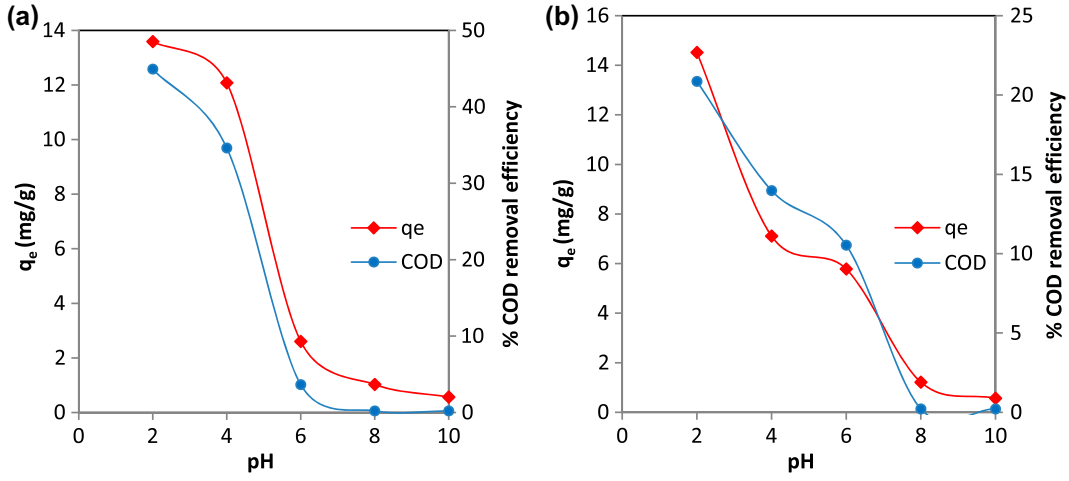

Fig. 7. The effect of pH on the dye and COD removal (a) Mt and (b) NMt (adsorbent dose = 0.1 g, contact time = 120 min for Mt and 20 min for NMt).

terazil) by activated carbon was taken place at pH 2 [45].

3.3.3. Effect of adsorbent dose

Fig. 8 present the influence of adsorbent dose (0.02 to 0.2 g) on NB and COD removal. As seen, by increasing the adsorbent dose from 0.01 to 0.2 g, the COD removal efficiency was increased from 20.9 to 62.2% for Mt and from 48.4 to 98.3% for NMt. These results are due to an increment of adsorbents contact surface and availability of more adsorption sites for dye molecules during the adsorption process [6,26]. But, NB loading capacity (amount of NB loaded per unit mass of the adsorbent) was gradually decreased with increasing the adsorbents dose (Fig. 8). The increase of dye loading capacity in lower amount of sorbent may be resulted from the accessibility of higher number of dye molecules per unit mass of the adsorbent (higher adsorbate/adsorbent ratio) [46].

3.3.3.1. Adsorption isotherms. Adsorption isotherms are used to distinguish the mechanism of adsorption process. The experimental data were fitted to the Freundlich, Langmuir, and Dubinin–Radushkevich (D–R) isotherm models. The Freundlich isotherm model is used to investigate the multilayer adsorption on a heterogeneous surface of adsorbent [16]. The linear form of Freundlich isotherm is defined by Eq. (6):

$$\ln q_e = \ln k_f + \frac{1}{n} \ln C_e \quad (6)$$

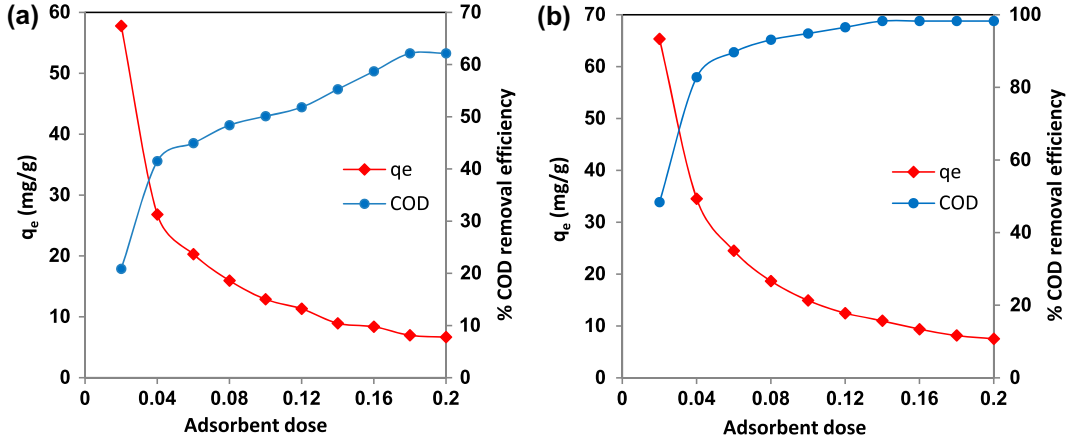

Fig. 8. The influence of (a) Mt and (b) NMt doses on the removal of dye and COD (dye solution volume = 100 mL, pH 2, contact time = 120 min for Mt and 20 min for NMt).

Table 4
Freundlich, Langmuir, and D–R isotherm parameters in dye sorption by Mt and NMt

	Freundlich isotherm			Langmuir isotherm			D–R isotherm		
Adsorbent	K_f (L/g)	n	R^2	q_m (mg/g)	b (L/mg)	R^2	q_m (mg/g)	E (kJ/mol)	R^2
Mt	1.819	0.68	0.94	35.21	0.07	0.92	39.06	0.389	0.92
NMt	4.609	0.53	0.97	28.09	0.18	0.97	136.67	0.465	0.97

where n and K_f (L/g) are the Freundlich isotherm constants which are the indicators of intensity and capacity of pollutant adsorption, respectively. The linear plotting ln q_e vs. ln C_e gives the intercept (K_f) and slop (n) [1]. Table 4 shows the Freundlich isotherm parameters for the adsorption of NB onto Mt and NMt. Langmuir isotherm model expresses monolayer adsorption of pollutant on a homogeneous surface of adsorbent sites [16,25]. Eq. (7) represents the linearized Langmuir isotherm.

$$\frac{C_e}{q_e} = \frac{C_e}{q_m} + \frac{1}{bq_m} \tag{7}$$

where q_e (mg/g) and C_e (mg/L) are the equilibrium adsorption capacity of adsorbent and dye concentration at equilibrium time, respectively, b (L/mg) is the equation constant, and q_m (mg/g) is the maximum adsorption capacity of adsorbent (monolayer) [1,23]. q_m and b can be obtained from the slope and intercept of linear plot of C_e/q_e against C_e, respectively. As seen from Table 4, the correlation coefficient (R^2) of the Freundlich, Langmuir, and D–R isotherm models for the dye sorption with NMt is higher than of Mt. So, the dye sorption with NMt was better fitted by the abovementioned isotherm models. The Freundlich isotherm fitted the experimental sorption data of Mt better than other isotherm models. But, the sorption data acquired by NMt were fitted well by the Freundlich and Langmuir isotherm models. The Freundlich isotherm constant, n, indicates the type of the adsorption process that it can be as chemical process ($n < 1$), linear ($n = 1$), and physical process ($n > 1$) [21,47]. The n values (0.68 for Mt and 0.53 for NMt) obtained from this isotherm model showed that NB removal by the adsorbents was as chemisorption. The D–R isotherm determines the adsorption type and the sorption mechanism as chemical or physical [48]. The D–R isotherm can be calculated using Eq. (8):

$$\ln q_e = \ln q_m - \beta\varepsilon^2 \tag{8}$$

where β (kJ/mol) is the equation constant (mean adsorption energy), q_m (mg/g) is the theoretical adsorption capacity, and ε is the Polanyi potential (calculates as $\varepsilon = RT.\ln(1 + 1/C_e)$). T (K) is temperature and R (kJ/mol k) is universal gas constant (8.314

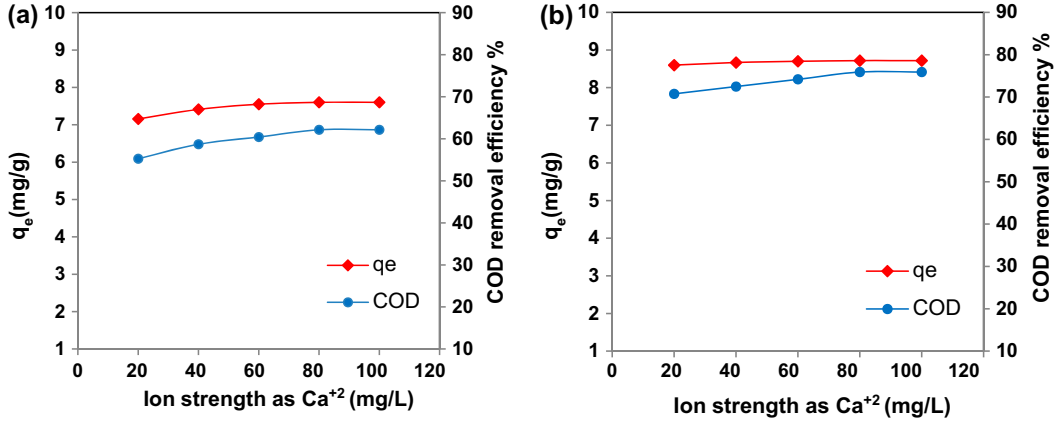

Fig. 9. The influence of ion strength on the adsorption of dye onto (a) Mt and (b) NMt (pH 2, adsorbent dose = 0.18 g, contact time = 120 min for Mt and 20 min for NMt).

J/mol k). q_m and β can be determined from the intercept and slope of linear plotting ln q_e vs. ε^2, respectively [1]. The mean adsorption energy (E) is achieved by Eq. (9):

$$E = \frac{1}{\sqrt{2\beta}} \quad (9)$$

The value of E (kJ/mol) determines the type of sorption mechanism [1,47]. The adsorption type can be explained as physical adsorption by $E < 8$ kJ/mol, while $E > 8$ kJ/mol displays the chemical adsorption. The chemical ion exchange can be played an important role in pollutant removal by E value between 8 and 16 kJ/mol [1]. As seen (Table 4), the E values of the dye adsorption via Mt (0.389 kJ/mol) and NMt (0.465 kJ/mol) showed that the sorption mechanism was as physical. Thus, in addition to chemical sorption (see interpretation of the Freundlich isotherm), the physical adsorption may be also occurred in the dye sorption process by Mt and NMt.

3.3.4. Effect of solution ion strength

To investigate the influence of solution ion strength on NB adsorption, $CaCl_2$ (20–100 mg/L of Ca^{+2} ions) was added to the dye solution. Fig. 9 illustrates the effect of solution ion strength on the adsorption capacity (q_e) and COD removal efficiency. As shown, increasing the solution Ca^{+2} ions had no negative effect on the dye and COD removal. Even, the COD removal was slightly increased by increasing the solution ion strength. This finding represents the good performance of the adsorbents in the different solution ion strengths. Pengthamkeerati et al. (2008) and De Souza et al. (2008) reported that the increment of solution ion strength has the partly positively effects on the dye sorption by other adsorbents [24,49].

3.4. Regeneration of dye-saturated adsorbent

Regeneration of spent adsorbent is an important factor to decrease the sorption system costs. Various solutions including sulfuric acid, acetic acid, sodium hydroxide, potassium hydroxide, ethanol along with ultrasonic, hot water and dry heating were applied to regenerate the dye-saturated adsorbents. The adsorption capacity of the regenerated Mt and NMt to the virgin adsorbents (q_e of regenerated sorbent/q_e of virgin sorbent) ratio is summarized in Table 5. As seen, the highest NB removal efficiency (RE%) was achieved by the adsorbents regenerated with sodium hydroxide (85.8% for Mt and 93.3% for NMt). According to Table 5, hot water and dry heating (300ºC) also had the acceptable regeneration efficiency.

Table 5
The regeneration efficiency (RE %) of Mt and NMt

Desorption agent	Mt (RE %)	NMt (RE %)
H_2SO_4	51.8	57.6
CH_3COOH	29.7	76.6
NaOH	85.8	93.3
KOH	41.9	75.8
Ultrasonic and ethanol	59.8	77.5
Hot water (95 ± 0.5°C)	81.0	83.3
Oven (300°C)	77.0	85.4

4. Conclusion

The decolorization and COD removal of a textile dye (NB) were surveyed from aqueous solutions by combined process of C–F and adsorption. Over the C–F process, commercial PACl at optimum pH 6 with a coagulant dose of 0.1 g/L was found to be the best coagulant among the other coagulants tested. The supernatant of C–F process was used in the adsorption step. The optimum conditions for the dye sorption were observed at pH 2 and the adsorbent dose 1.8 g/L. The adsorption capacity and COD removal efficiency of Mt and NMt at equilibrium time (120 min for Mt and 20 min for NMt) were 8.93 mg/g, 41.51% and 8.87 mg/g, 19.14%, respectively. The results of sorbent regeneration experiments also showed that the highest NB removal efficiency (RE%) was achieved by the adsorbents regenerated with sodium hydroxide. The dye and COD concentrations during the combined treatment process were decreased from 300 to 2–4.5 mg/L and from 732 to 2–35 mg/L, respectively. This indicates that C–F followed by adsorption techniques can be considered as an excellent alternative for the treatment of NB containing wastewaters.

Acknowledgements

This research, as MSc thesis, was financially supported by the vice chancellery of research of Isfahan University of Medical Sciences, Iran (grant number 392130). The authors are grateful to Eng. M. Vahid Dastjerdi and Dr Mohsen Sadani from Isfahan University of Medical Sciences for their guidance and technical support.

References

[1] H. Nourmoradi, M. Khiadani, M. Nikaeen, Multi-Component adsorption of benzene, toluene, ethylbenzene, and xylene from aqueous solutions by montmorillonite modified with tetradecyl trimethyl ammonium bromide, E-J. Chem. 2013 (2013) 1–10.
[2] V. Vimonses, B. Jin, C.W.K. Chow, C. Saint, Development of a pilot fluidised bed reactor system with a formulated clay–lime mixture for continuous removal of chemical pollutants from wastewater, Chem. Eng. J. 158 (2010) 535–541.
[3] S.Y. Wong, Y.P. Tan, A.H. Abdullah, S.T. Ong, The removal of basic and reactive dyes using quartenised sugar cane bagasse, J. Phys. Sci. 20 (2009) 59–74.
[4] H.R. Guendy, Treatment and reuse of wastewater in the textile industry by means of coagulation and adsorption techniques, J. Appl. Sci. Res. 6 (2010) 964–972.
[5] X. Jin, M.-Q. Jiang, X.-Q. Shan, Z.-G. Pei, Z. Chen, Adsorption of methylene blue and orange II onto unmodified and surfactant-modified zeolite, J. Colloid Interface Sci. 328 (2008) 243–247.
[6] E. Gutiérrez-Segura, M. Solache-Ríos, A. Colín-Cruz, Sorption of indigo carmine by a Fe-zeolitic tuff and carbonaceous material from pyrolyzed sewage sludge, J. Hazard. Mater. 170 (2009) 1227–1235.
[7] F. El-Gohary, A. Tawfik, Decolorization and COD reduction of disperse and reactive dyes wastewater using chemical–coagulation followed by sequential batch reactor (SBR) process, Desalination 249 (2009) 1159–1164.
[8] M. Turabik, Adsorption of basic dyes from single and binary component systems onto bentonite: Simultaneous analysis of Basic Red 46 and Basic Yellow 28 by first order derivative spectrophotometric analysis method, J. Hazard. Mater. 158 (2008) 52–64.
[9] K.E. Lee, T.T. Teng, N. Morad, B.T. Poh, M. Mahalingam, Flocculation activity of novel ferric chloride–polyacrylamide ($FeCl_3$-PAM) hybrid polymer, Desalination 266 (2011) 108–113.
[10] T.H. Kim, C. Park, J. Yang, S. Kim, Comparison of disperse and reactive dye removals by chemical coagulation and Fenton oxidation, J. Hazard. Mater. 112 (2004) 95–103.
[11] R. Sivaraj, R. Venckatesh, G. Gowri Sangeetha, Activated carbon prepared from *Eichornia crassipes* as an adsorbent for the removal of dyes from aqueous solution, Int. J. Eng. Sci. Technol. 2 (2010) 2418–2427.
[12] M. Riera-Torres, C. Gutiérrez-Bouzán, M. Crespi, Combination of coagulation–flocculation and nanofiltration techniques for dye removal and water reuse in textile effluents, Desalination 252 (2010) 53–59.
[13] T.H. Kim, C. Park, E.-B. Shin, S. Kim, Decolorization of disperse and reactive dye solutions using ferric chloride, Desalination 161 (2004) 49–58.
[14] E. Demirbas, M.Z. Nas, Batch kinetic and equilibrium studies of adsorption of Reactive Blue 21 by fly ash and sepiolite, Desalination 243 (2009) 8–21.
[15] B. Hayati, N.M. Mahmoodi, M. Arami, F. Mazaheri, Dye removal from colored textile wastewater by poly (propylene imine) dendrimer: Operational parameters and isotherm studies, Clean Soil, Air, Water 39 (2011) 673–679.
[16] V. Vimonses, B. Jin, C.W.k. Chow, Insight into removal kinetic and mechanisms of anionic dye by calcined clay materials and lime, J. Hazard. Mater. 177 (2010) 420–427.
[17] P. Kumar, B. Prasad, I.M. Mishra, S. Chand, Decolorization and COD reduction of dyeing wastewater from a cotton textile mill using thermolysis and coagulation, J. Hazard. Mater. 153 (2008) 635–645.
[18] L. Semerjian, G.M. Ayoub, High-pH–magnesium coagulation–flocculation in wastewater treatment, Adv. Environ. Res. 7 (2003) 389–403.
[19] A. Zahrim, C. Tizaoui, N. Hilal, Coagulation with polymers for nanofiltration pre-treatment of highly concentrated dyes: A review, Desalination 266 (2011) 1–16.
[20] J. Fan, A. Li, W. Yang, L. Yang, Q. Zhang, Adsorption of water-soluble dye X-BR onto styrene and acrylic ester resins, Sep. Purif. Technol. 51 (2006) 338–344.
[21] V. Vimonses, S. Lei, B. Jin C.W.k. Chow C. Saint, Kinetic study and equilibrium isotherm analysis of Congo Red adsorption by clay materials, Chem. Eng. J. 148 (2009) 354–364.

[22] G. Zhang, X. Li, Y. Li, T. Wu, D. Sun, F. Lu, Removal of anionic dyes from aqueous solution by leaching solutions of white mud, Desalination. 274 (2011) 255–261.
[23] H. Faghihian, H. Nourmoradi, M. Shokouhi, Removal of copper (II) and nickel (II) from aqueous media using silica aerogel modified with amino propyl triethoxysilane as an adsorbent: Equilibrium, kinetic and isotherms study, Desalin. Water Treat. 52 (2013) 305–313.
[24] P. Pengthamkeerati, T. Satapanajaru, O. Singchan, Sorption of reactive dye from aqueous solution on biomass fly ash, J. Hazard. Mater. 153 (2008) 1149–1156.
[25] P.K. Malik, Dye removal from wastewater using activated carbon developed from sawdust: Adsorption equilibrium and kinetics, J. Hazard. Mater. 113 (2004) 81–88.
[26] V. Vimonses, B. Jin C.W.k. Chow C. Saint, Enhancing removal efficiency of anionic dye by combination and calcination of clay materials and calcium hydroxide, J. Hazard. Mater. 171 (2009) 941–947.
[27] S.H. Lin, R.-S. Juang, Y.-H. Wang, Adsorption of acid dye from water onto pristine and acid-activated clays in fixed beds. J. Hazard. Mater. 113 (2004) 195–200.
[28] S. Papic, N. Koprivanac, A.L. Bozic, A. Metes, Removal of some reactive dyes from synthetic wastewater by combined Al(III) coagulation/carbon adsorption process, Dyes Pigments 62 (2004) 291–298.
[29] J.W. Lee, S.-P. Choi, R. Thiruvenkatachari, W.-G. Shim, H. Moon, Evaluation of the performance of adsorption and coagulation processes for the maximum removal of reactive dyes, Dyes Pigments 69 (2006) 196–203.
[30] F.R.Furlan, L.G.M. de Melo da Silva, A.F.Morgado, A.A.U.de Souza, S.M.A.G.U Guelli Ulson de Souza, Removal of reactive dyes from aqueous solutions using combined coagulation/flocculation and adsorption on activated carbon, Resour. Conserv. Recy. 54 (2010) 283–290.
[31] F. Harrelkas, A. Azizi, A. Yaacoubi, A. Benhammou, M.N. Pons, Treatment of textile dye effluents using coagulation–flocculation coupled with membrane processes or adsorption on powdered activated carbon, Desalination 235 (2009) 330–339.
[32] APHA, WEF, AWWA, Standard methods for the examination of water and wastewater, twenty-first edition, American Public Health Association, Washington, D.C. 2005.
[33] W.P. Wen, T.T. Tow, Z.M. Zain, Removal of disperse dye and reactive dye by coagulation-flocculation method (2003). Available from http://eprints.usm.my/6901.
[34] Y.-Z. Wen, S.-P. Tong, K.-F. Zheng, L.-L. Wang, J.-Z. Lv, J. Lin, Removal of terephthalic acid in alkalized wastewater by ferric chloride, J. Hazard. Mater. 138 (2006) 169–172.
[35] L. Ravina, N. Moramarco, Everything you want to know about coagulation & flocculation, Zeta-Meter Inc, Staunton, 1993.
[36] F. Ying, G. Bao-yu, Z. Yi-feng, Z. Xin-yu, S. Nan, Organic modifier of poly-silicic-ferric coagulant: Characterization, treatment of dyeing wastewater and floc change during coagulation, Desalination 277 (2011) 67–73.
[37] P.V. Nidheesh, R. Gandhimathi, S.T. Ramesh, T.S.A. Singh, Adsorption and desorption characteristics of crystal violet in bottom as holumn, J. Urban Environ. Eng. 6 (2012) 18–29.
[38] A.S. Alimmari, A.D. Marinković, D.Ž. Mijin, N.V. Valentić, N. Todorović, G.S. Uščumlić, Synthesis, structure and solvatochromic properties of 3-cyano-4,6-diphenyl-5-(3-and 4-substituted phenylazo)-2-pyridones, J. Serb. Chem. 75 (2010) 1019–1032.
[39] C.W.M. Yuen, S.K.A. Ku, P.S.R. Choi, C.W. Kan, S.Y. Tsang, Determining functional groups of commercially available ink-jet printing reactive dyes using infrared spectroscopy, Res. J. Text. Appar. 9 (2005) 26–38.
[40] M.R. Derrick, D. Stulik, J.M. Landry, Infrared Spectroscopy in Conservation Science, Getty Publications, New York, NY, 2000.
[41] G.M. Malik, S.K. Zadafiya, Thaizole based disperse dyes and their dyeing application on polyester fiber and their antimicrobial activity, Chem. Sin. 1 (2010) 15–21.
[42] Y. Li, B. Gao, T. Wu, B. Wang, X. Li, Adsorption properties of aluminum magnesium mixed hydroxide for the model anionic dye Reactive Brilliant Red K-2BP, Chem. Sin. 164 (2009) 1098–1104.
[43] Y.S. Ho, C.C. Chiang, Sorption studies of acid dye by mixed sorbents, Adsorption 7 (2001) 139–147.
[44] H. Nourmoradi, A. Ghiasvand, Z. Noorimotlagh, Removal of methylene blue and acid orange 7 from aqueous solutions by activated carbon coated with zinc oxide (ZnO) nanoparticles: Equilibrium, kinetic, and thermodynamic study, Desalin. Water Treat. (2014) 1–11. doi:10.1080/19443994.2014.914449.
[45] S. Hemsas, H. Lounici, Z. Belkebi, Kh Benrachedi, Removal of dispersed dyes from aqueous solution using activated carbon prepared from olive stones, JAST. A 4 (2014) 414–421.
[46] S.P. Kamble, P.A. Mangrulkar, A.K. Bansiwal, S.S. Rayalu, Adsorption of phenol and *o*-chlorophenol on surface altered fly ash based molecular sieves, Chem. Eng. J. 138 (2008) 73–83.
[47] A.S. Özcan, B. Erdem, A. Özcan, Adsorption of Acid Blue 193 from aqueous solutions onto BTMA-bentonite, Colloids Surf., A 266 (2005) 73–81.
[48] S.K. Maji, A. Pal, T. Pal, A. Adak, Adsorption thermodynamics of arsenic on laterite soil, J. Surface Sci. Technol. 22 (2007) 161–176.
[49] S.M.A. Guelli U. de Souza, M. Selene L.C. Peruzzo, Numerical study of the adsorption of dyes from textile, Appl. Math. Model. 32 (2008) 1711–1718.